

# TRIBO-ELECTROCHEMICAL BEHAVIOR OF A FERRITIC STAINLESS STEEL UNDER APPLIED POTENTIALS.

V. Dalbert<sup>1</sup>, N. Mary<sup>1</sup>, C. Verdu<sup>1</sup>, H. N. Evin<sup>2</sup>, B. Normand<sup>1</sup>

<sup>1</sup> Université de Lyon, INSA-Lyon, MATEIS CNRS UMR 5510, 69621 Villeurbanne, France

<sup>2</sup> APERAM Research Center, rue Roger Salengro BP15, F-62330 Isbergues, France

**Abstract:** A tribo-electrochemical characterization of a ferritic stainless steel has been carried out under reciprocating sliding against a corundum alumina pin in 0.02 M H<sub>2</sub>SO<sub>4</sub> medium at room temperature. The aim of this study is to present a refinement of the usually employed method to determine the synergism effect occurring in a tribo system where the sample is made of passive metal and the counter body made of inert material. The effects of mechanical, corrosion and synergistical contributions to tribocorrosion at each investigated potential are discriminated. So as to further study the synergy, it is divided into two parts, electrochemistry-accelerated wear (EAW) and wear-accelerated electrochemistry (WAE), respectively. Focus is first addressed on the mechanical wear reference determination under cathodic polarization. It has been shown that depending on the selected cathodic potential a hydrogen effect or even a dissolution contribution could result in EAW contribution of about 60% of the overall degradation. These effects are avoided when polarization is made at a potential where the double layer thickness is maximum and could serve as lubricant agent under friction. The wear volume found under these conditions could therefore be used as mechanical wear reference. In the anodic domain, with the employed set-up, it is possible to set an idle time long enough for the film to reform between each sliding. Charges released during pin motions periods are thus related to depassivation process only and are converted into WAE wear volumes using the Faraday's law. Wear volumes are quite constant over the investigated range in the passive plateau. They are more important than what is observed at lower potentials because of great EAW wear volumes. However, the proportions of wear contributions to the overall material degradation are changing. Even if the mechanical contribution is quite constant over the considered passive range around 23%, a transfer is occurring from the EAW contribution to the WAE one as the anodic potential is increased.

**Keywords:** ferritic stainless steel; tribocorrosion; mechanical wear reference; synergy

## 1 INTRODUCTION

Ferrite stainless steels are widely used to fight corrosion thanks to their native protective passive film [1]. Given their application fields and aggressive environments under operating conditions, it is important to follow a multifunctional approach linking both friction and physicochemistry to deal with corrosion. It is now well accepted that the simultaneity of these phenomena leads to tribocorrosion [2]. Indeed, tribocorrosion is a phenomenon which appears when two contacting bodies are in relative motion in a corrosive medium. In this configuration, wear induced by sliding and corrosion separately taken from each other is increased because of combined effects. These interaction effects are particularly significant for passive stainless steels when the protective feature of the passive film is lost under the mechanical load within the contact.

The first step to assess the tribocorrosion resistance is to determine the total wear. The second step is to discriminate the mechanical contribution from the corrosion one in this overall damage. In several parametric studies, ferritic stainless steels present a greater wear and highest current values under more severe sliding conditions [3,4]. Thus, wear was divided into two contributions between mechanical wear and electrochemical wear, the latter standing for the corrosion of the worn and unprotected surface [5]. This approach was followed under sliding in acidic medium [4]. The electrochemical contribution is there related to the tribocorrosion current whereas the mechanical contribution is obtained as the difference between global wear and the electrochemical contribution.

Nonetheless another approach can be selected to highlight the synergism effect occurring in tribocorrosion. To improve its physical meaning, the synergy is further divided into two parts, electrochemistry-accelerated wear (EAW) and wear-accelerated electrochemistry (WAE), respectively [6]. The synergistical contribution is here the difference between the global wear and both the pure corrosion wear and the mechanical reference. From a chemical point of view, the mechanical wear reference can be investigated in distilled water or in presence of corrosion inhibitors [7] but the tribosystem chemistry becomes different. With an electrochemical approach, experiments have to be done under cathodic polarization where the sample surface is expected to be free from oxide and dissolution processes [8]. It usually consists in an arbitrary

choice where hydrogen reduction [9] or material dissolution could lead to an overestimation of the mechanical contribution to wear. Systematic wear determination at different applied cathodic potentials could be done in order to select the relevant potential [7,9,10]. Nonetheless a more fundamental approach based on double layer lubrication properties [11] could avoid such screening method.

The aim of this study is to present a refinement of the usually employed method to determine the synergism effect in a tribosystem where the sample is made of passive metal and the counter body made of inert material. Results will be given on a commercial ferritic stainless steel. Focus will be addressed first on the mechanical wear reference determination under cathodic polarization and then on synergism effect evolution with the applied anodic overpotential.

## 2 EXPERIMENTAL PROCEDURE

### 2.1 Materials

This work was carried out on a 16 wt-% Cr commercial ferritic stainless steel. The yield strength  $R_{p0.2}$  is 290 MPa, the tensile strength  $R_m$  is 580 MPa and the strain at fracture  $A$  is 29%. Its Young modulus and Poisson ratio are taken as 220 GPa and 0.3, respectively. On the microstructure, revealed by electrochemical etching, grains do not show any rolling orientation (Figure 1).

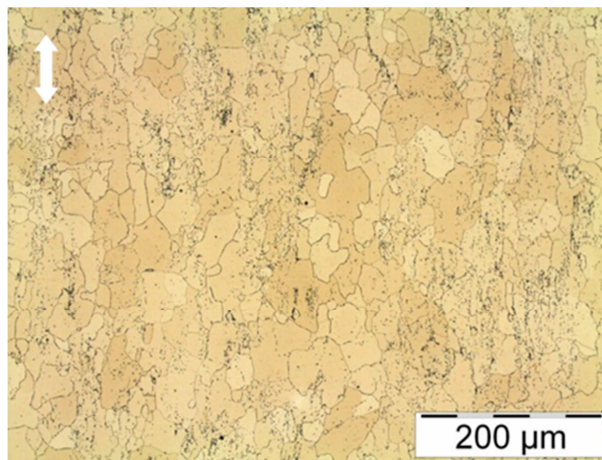


Figure 1. Microstructure of the ferritic stainless steel after an electrochemical etching. Dark dots over the surface are chromium carbides. The arrow indicates the rolling direction.

Before electrochemical and tribocorrosion experiments, samples were polished up to 1  $\mu\text{m}$  diamond paste, cleaned in an ethanol ultrasonic bath for 1 minute, dried with pulsed dry air and stored in a desiccator during 24h for film ageing. Corundum alumina pin with a 25 mm curvature radius was selected as counter body because of its chemical and mechanical resistance (Young modulus and Poisson ratio of 380 GPa and 0.25, respectively).

### 2.2 Experimental setup

Electrochemical experiments were performed using a potentiostat (Gamry, REF600) in a classical three electrodes tribo-cell. Working electrodes consisted in polished ferritic stainless steel samples with active surfaces of 10.17  $\text{cm}^2$ . A graphite disc played the role of the counter electrode (surface of 16  $\text{cm}^2$ ). The potentials were recorded versus a mercury sulfate electrode ( $E_{\text{MSE}} = +650 \text{ mV/SHE}$ ). The medium was a 0.02 M  $\text{H}_2\text{SO}_4$  aerated solution at room temperature.

Tribocorrosion tests were performed using a reciprocating motion tribometer (Falex). Contact features of this sphere-on-plane configuration are calculated according to Hertz assumptions. With a nominal load of 10 N, the pin impression on the surface is estimated at 460 nm, much greater than a typical passive film thickness of 3-4 nm [1]. The Hertz contact stiffness is calculated at  $3.25 \times 10^7 \text{ N/m}$  with a maximum Hertz contact stress of 414 MPa. Since this value is greater than  $R_{p0.2}$ , plastic deformation is expected. Experiments were carried out during 1000 cycles with a 10 mm sliding distance. The motion type was trapezoidal with an acceleration of 500  $\text{mm/s}^2$  and a maximum velocity of 50  $\text{mm/s}$ . The forward and the backward holding times were set at 5 s in order to get current stability and oxi-hydroxide film regrowth between two successive scratches.

### 2.3 Experiments

In order to increase tests reproducibility, a cathodic potential of -1.05 V/MSE was applied for 30 min prior to any electrochemical or tribo electrochemical experiment. Polarization curves were recorded from -1.100 to

+0.300 V/MSE with a scan rate of 0.5 mV/s to characterize the passivation behavior of the ferritic stainless steel and select the applied potentials. Since hydrogen reduction or anodic current close to the corrosion potential could affect the double layer features [11] as well as the mechanical degradation in the cathodic domain [9], a high frequency stimulation of the sample was carried out from -0.950 to -1.400 V/MSE with 10 mV steps [12]. The AC amplitude and frequency were fixed at 5 mV RMS and 500 Hz, respectively.

For tribocorrosion experiments, the selected potential is applied for 4.5 h. After 10 minutes of polarization to stabilize either cathodic or anodic reactions, sliding is performed. After the experiments completion, samples were cleaned with distilled water and dried. No corrosion products were found on the sample surface. Contact profilometry (Somicronic, Surfscan 2D) was performed to get crosssectional areas in the middle of the wear track. Averaged crosssectional areas values were used to calculate the total wear volume schematized as a central semi-cylindrical part with semi-spherical portions at the ends. Finally, secondary electron microscopy (Zeiss, Supra 55VP) was used to investigate the wear track morphology at each potential.

### 3 RESULTS AND DISCUSSION

#### 3.1 Electrochemical behavior

##### 3.1.1 Anodic applied potentials selection from the polarization curve

The representative polarization curve is shown with a corrosion potential at -0.930 V/MSE (Figure 2). Above -0.710 V/MSE, a passive plateau is observed with a current density below  $10 \mu\text{A}/\text{cm}^2$ . In order to evaluate the electromechanical wear versus the film growth potential, two anodic values were chosen within the passive plateau at -0.710 and -0.050 V/MSE. Olefjord and Wegrelius showed that the thickening of the oxide is potential dependent in the passive plateau [13]: the greater the passive potential, the greater the oxide growth driving force. Thus the oxide part of the oxi-hydroxide film will be thicker under -0.050 V/MSE than under -0.710V/MSE.

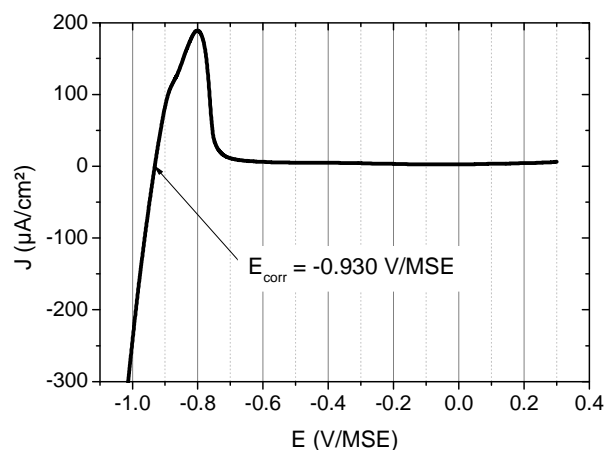


Figure 2. Polarization curve of the ferritic stainless steel after the cathodic reduction.

##### 3.1.2 Cathodic applied potentials selection from the double layer evolution

To select cathodic potentials for the mechanical reference determination, the double layer capacity is plotted as a function of the cathodic potential and shows a minimum between -1.200 and -1.000 V/MSE (Figure 3). On this plateau, water molecules are expected to adsorb most strongly, this is the Potential of Zero Charge (PZC) [14]. As the capacity of the double layer is inversely proportional to its thickness, the latter reaches its maximum at PZC. The influence of thick and strongly adsorbed water molecules layers onto the surface could reduce the friction coefficient thanks to a lubrication effect [11].

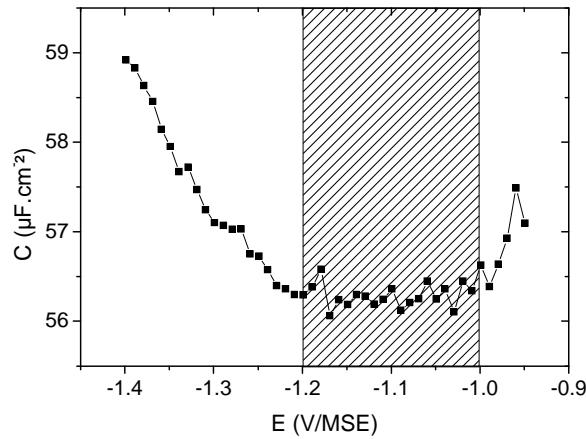


Figure 3. Double layer capacity evolution as a function of the applied potential.

For potentials higher than  $-1.000$  V/MSE, the double layer capacity increases because sulfate anions will be attracted to the surface according to the PZC approach [12,14]. Close to the corrosion potential, the dissolution contribution becomes not negligible. For potentials lower than  $-1.200$  V/MSE, the double layer capacity increases because of proton attraction and adsorption onto the surface [12,14]. With a high cathodic potential, hydrogen reduction is promoted.

Finally, wear reference determination has to be done in the potential range of  $-1.200$  to  $-1.000$  V/MSE with selected potentials at  $-1.200$  and  $-1.050$  V/MSE. Another cathodic value outside this range ( $-0.950$  V/MSE) is also investigated for comparison purposes.

### 3.2 Total wear volumes and wear behavior under applied potentials

Tribo-electrochemical tests were performed under either cathodic or anodic potentials. Results consist in friction coefficients and wear volumes determination (Table 1). For each experiment, no debris was revealed by SEM observations and corundum pins did not show any wear or third body transfer.

Table 1. Friction coefficients and total wear volumes as a function of the applied potential. 1000 cycles of sliding under a 10 N load.

	Applied potential (V/MSE)	Friction coefficient	Wear volume $V_{tot}$ ( $10^{-3} \cdot \text{mm}^3$ )
Cathodic domain	-1.200	$0.67 \pm 0.06$	$25.7 \pm 1.0$
	-1.050	$0.57 \pm 0.12$	$8.9 \pm 0.4$
	-0.950	$0.79 \pm 0.07$	$20.7 \pm 0.6$
Passive domain	-0.710	$0.57 \pm 0.05$	$40.5 \pm 7.7$
	-0.050	$0.72 \pm 0.14$	$35.7 \pm 5.3$

#### 3.2.1 Under cathodic applied potentials

Minimum of wear ( $8.9 \times 10^{-3} \text{ mm}^3$ ) is found at  $-1.050$  V/MSE. Sliding conditions are characterized by a rather low friction coefficient at 0.57. This is related to the double layer capacity approach where adsorbed water molecules on the surface may act as a lubricant. SEM micrograph of the worn surface reveals numerous and homogeneously distributed dimples (Figure 4).

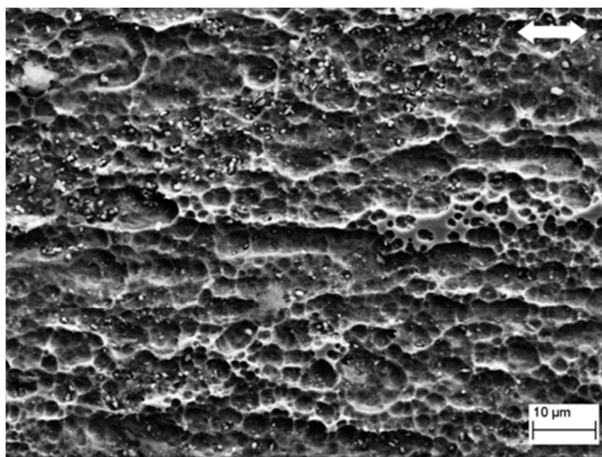


Figure 4. Scanning electron micrograph in the middle of the wear track after a test carried out at -1.050V/MSE. The arrow indicates the sliding direction.

Wear values at -1.200 and -0.950 V/MSE become significantly higher with  $25.7 \times 10^{-3} \text{ mm}^3$  and  $20.7 \times 10^{-3} \text{ mm}^3$ , respectively. On the one hand, at -1.200 V/MSE, a sparging is observed in the wear track. Sliding could promote the hydrogen reduction according to the previous PZC analysis. The gas bubbles in the wear track will modify the contact conditions between the pin and the surface turning it into a partially dry mode. This increases the friction coefficient up to 0.67. Therefore, the lubricant effect of the double layer, expected in static conditions, will not occur in dynamic conditions. On the other hand, at -0.950 V/MSE, a dissolution contribution takes place because of the corrosion potential vicinity (-0.930 V/MSE). It is promoted by the sulfate adsorption according to the PZC analysis.

These analyses highlight that the double layer capacity measurement can be used to select the cathodic potentials for the mechanical wear reference determination. Because of pin motion, the hydrogen reduction changes the contact mode and increases the wear. Dissolution processes increased the wear at -0.950 V/MSE, as expected. Finally, the wear found at -1.050 V/MSE is taken as mechanical wear reference.

### 3.2.2 Under anodic applied potentials

In the passive plateau, the friction coefficient increases with the potential from -0.710 V/MSE to -0.050 V/MSE. It is linked to the mechanical resistance of a thicker oxide layer [4,15]. In the meantime, the wear volume decreases. These observations are consistent with results obtained in more acidic solutions [3].

At -0.710 V/MSE, the surface is smooth and uniform with numerous scratches (Figure 5a) whereas SEM observation exhibits a non-uniform wear track with oxide detachment at -0.050 V/MSE (Figure 5b). The smoother surface at -0.710 V/MSE may be explained by a thinner and weaker oxide that could be easier to smear over the wear track.

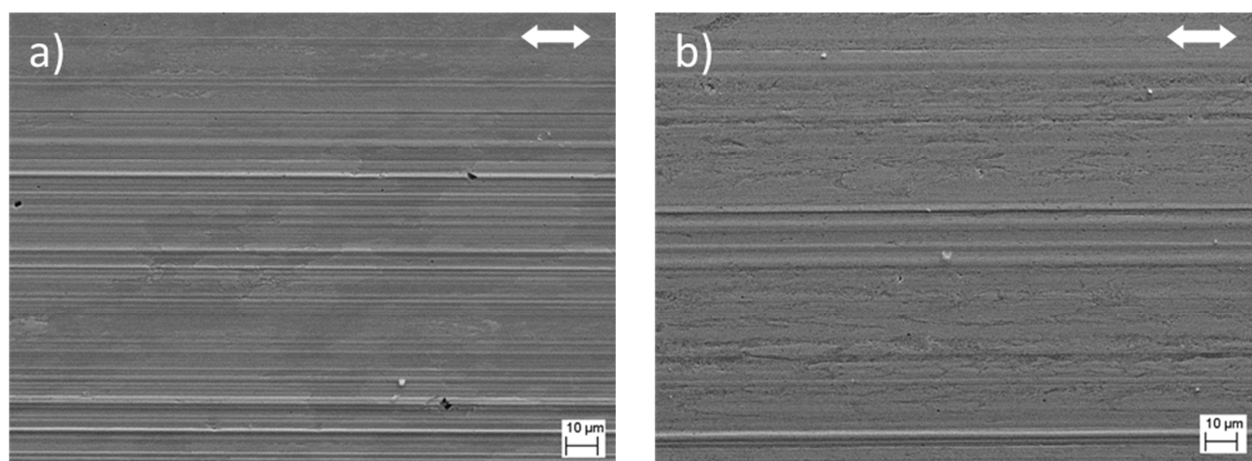


Figure 5. Scanning electron micrographs inside the wear track at a) -0.710 V/MSE and b) -0.050 V/MSE. Arrows indicate the sliding direction.

### 3.3 Wear-accelerated electrochemistry (WAE) wear volumes determination under anodic potentials

A base current (named  $I_{base}$ ) is observed when no sliding is performed and stands for passive film formation (Figure 6a). Since it is very low, it is neglected as well as the resulting pure corrosion wear volume.

An increase of the measured current is observed under sliding (Figure 6a). For instance, at  $-0.050$  V/MSE, the sharp current increase within the first 500 seconds is due to the running-in step before reaching a plateau at  $1.75$  mA as wear is in stabilized regime. At the end of sliding, current drops back to its initial and low values ( $I_{base}$ ).

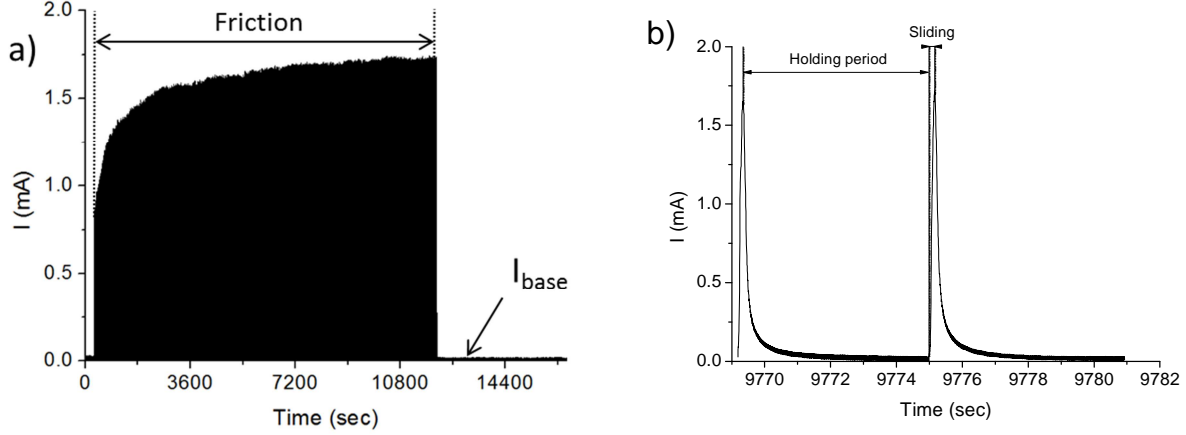


Figure 6. Measured current versus time plot for the experiment performed at  $-0.050$  V/MSE over a) the entire experiment and b) a short acquisition period.

During sliding, the friction current is calculated as the difference between the measured current and the base current with Eq. (1).

$$I_{friction} = I_{measured} - I_{base} \quad (1)$$

The friction current transients can be decomposed into two parts linked to the reciprocating motion (Figure 6b). First, a fast current increase related to sliding is observed. Garcia et al. showed that a mechanical load threshold exists for the film removal [16]. Below this value, only a film thinning occurs. However, above this value, the film is completely removed by the pin. The mechanical parameters used in this work leads to consider the latter case. An oxide free surface is thus generated and the friction current increase is related to oxidation processes. During the idle period however, the friction current decrease is attributed to the passive film healing.

Only charges related to pin motion periods have to be considered in the material degradation. They stand for WAE and are calculated by integrating the friction current over the sliding period for each (i) sliding ( $Q_{friction,i}$  in Eq. (2)) [10,17].

$$Q_{friction,i} = \int_{start,i}^{stop,i} I_{friction,i}(t) dt \quad (2)$$

Cumulated friction charges may be calculated over the entire experiment ( $Q_{friction}$ ) using Eq. (3) and converted into WAE wear volumes ( $V_{wae}$ ) with the Faraday's law (Eq. (4)).

$$Q_{friction} = \sum_i Q_{friction,i} \quad (3)$$

$$V_{wae} = \frac{Q_{friction} * M_{eq}}{n_{eq} * F * \rho} \quad (4)$$

$F$  is the Faraday constant ( $96500$  C/mol) and  $\rho$  the alloy density ( $7.7$  g/cm<sup>3</sup>).  $M_{eq}$  is the equivalent molar weight of the alloy given by  $M_{eq} = X_{Fe}M_{Fe} + X_{Cr}M_{Cr}$  where  $X_i$  are the molar fractions and  $M_i$  the molar weights of the major alloying elements. According to the chemical composition of the stainless steel,  $M_{eq}$  is equal to  $55.18$  g/mol. Assuming that only iron and chromium are dissolved to form  $Fe^{2+}$  and  $Cr^{3+}$  cations respectively, the alloy equivalent charge number,  $n_{eq}$ , is estimated to  $2.17$  with  $n_{eq} = X_{Fe}n_{Fe} + X_{Cr}n_{Cr}$  where  $X_i$  are the molar fractions and  $n_i$  the charge numbers of the main alloying elements.

Table 2. WAE wear volumes as a function of the applied potential. 1000 cycles of sliding under a 10 N load.

	Applied potential (V/MSE)	WAE wear volume $V_{wae}$ ( $10^{-3}$ .mm <sup>3</sup> )
Passive domain	-0.710	$2.7 \pm 0.5$
	-0.050	$8.4 \pm 0.9$

Results are summarized in Table 2. Contrary to the literature [3,4], current values and thus WAE wear volumes are increasing with higher passive potentials. It could be explained by stronger oxidative reactions taking place at higher passive potential on the bare metal exposed by sliding to the electrolyte.

### 3.4 Electrochemistry-accelerated wear (EAW) wear volumes determination under anodic potentials

The total wear volume ( $V_{tot}$ ) is the sum of the mechanical, corrosion and synergistical wear volumes ( $V_m$ ,  $V_{corr}$  and  $V_s$ , respectively). So as to further study the synergy, it is decomposed into WAE and EAW [6] and their associated wear volumes ( $V_{wae}$  and  $V_{eaw}$ , respectively). This leads to Eq. (5).

$$V_{tot} = V_m + V_{corr} + V_{wae} + V_{eaw} \quad (5)$$

The pure chemical wear is neglected since a passivable material is studied within its passive range.  $V_{wae}$  is calculated as previously explained and is related to electrochemical processes occurring on a generated fresh surface.  $V_{eaw}$  quantifies the wear due to modified surface mechanical properties induced by electrochemistry and is determined using Eq. (6).

$$V_{eaw} = V_{tot} - V_m - V_{wae} \quad (6)$$

As discussed above, the mechanical wear reference is found at -1.050 V/MSE and its value is taken as mechanical wear volume whatever the applied potential considered (Figure 7a). Wear components proportions are calculated to highlight the effect of each contribution to wear (Figure 7b).

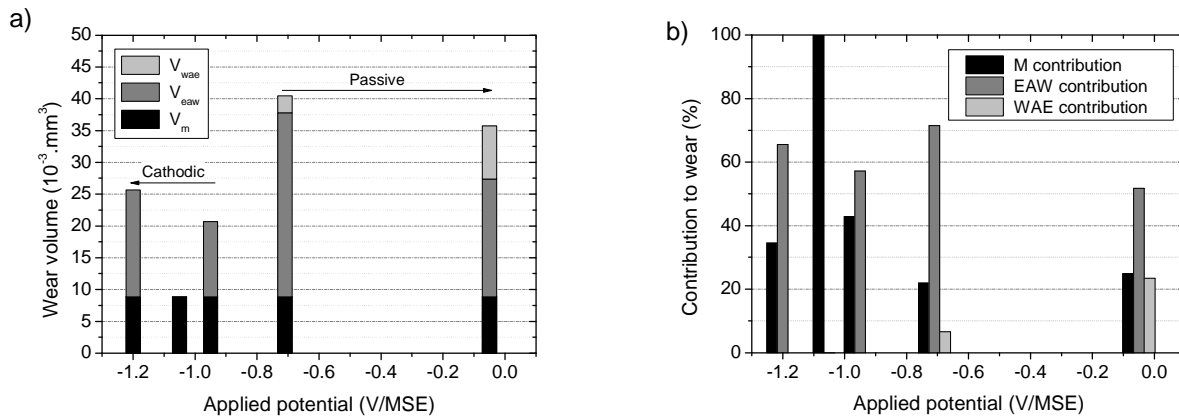


Figure 7. a) Wear volumes composition and b) proportion of contributions to wear as a function of the applied potential.

Under cathodic potentials, the total wear volume is affected either by a hydrogen evolution at -1.200 V/MSE or by a dissolution contribution at -0.950 V/MSE. In both cases the EAW contribution to wear stands for around 60% of the overall degradation. It is thus all the more important for tribocorrosion studies to carefully select the cathodic potential used to determine the pure mechanical wear.

Within the passive plateau, the total degradation is more important than out of this potential range because of great EAW wear volumes. The mechanical contribution is quite constant around 23%. However as the potential is increased, the EAW contribution decreases from 72% at -0.710 V/MSE to 52% at -0.050 V/MSE. The thicker oxide grown under higher passive potential could more protect the surface under mechanical load. In the meantime, the WAE contribution increases from 7% to 23%. A transfer is occurring from the EAW contribution to the WAE one as the anodic potential is increased.

## 4 CONCLUSIONS

A tribo-electrochemical characterization of a ferritic stainless steel has been carried out under reciprocating sliding against an alumina pin in 0.02 M  $\text{H}_2\text{SO}_4$  medium at room temperature.

This study is based, under cathodic potentials, on determining the mechanical wear reference. It has been shown that the minimum wear is obtained when sliding is performed at the potential for zero charge (-1.050 V/MSE) where the double layer could play the role of a lubricant. Other phenomena such as hydrogen reduction (-1.200 V/MSE) or hidden dissolution processes (-0.950 V/MSE) contribute up to around 60% to the overall degradation. Care should therefore be taken to choose the potential used for the mechanical wear reference determination.

Under passive potentials, an idle period, long enough for the metal to repassivate between two consecutive scratches is compulsory to discriminate the charges released during repassivation and those released during depassivation. Only the latter are considered for WAE wear volumes calculations. Because of great EAW wear volumes, wear is greater over the passive plateau with a slight decreasing trend observed from -0.710 to -0.050 V/MSE. However, the proportions of the different contributions to wear are changing. By considering the mechanical contribution (around 23%) constant within the passive range, the EAW contribution diminishes whereas the WAE one grows as the anodic potential is increased.

## 5 ACKNOWLEDGEMENTS

The authors would like to acknowledge the technical support of R. Di-Folco, R. Diemiaszonek and A. Gaugain.

## 6 REFERENCES

- [1] C.O.A. Olsson et D. Landolt, Passive films on stainless steels—chemistry, structure and growth, *Electrochimica Acta*, vol. 48, n° 9, p. 1093-1104, 2003.
- [2] D. Landolt, Electrochemical and materials aspects of tribocorrosion systems, *Journal of Physics D: Applied Physics*, vol. 39, n° 15, p. 3121-3127, 2006.
- [3] M. Stemp, S. Mischler, et D. Landolt, The effect of mechanical and electrochemical parameters on the tribocorrosion rate of stainless steel in sulphuric acid, *Wear*, vol. 255, n° 1-6, p. 466-475, 2003.
- [4] P. Jemmely, S. Mischler, et D. Landolt, Tribocorrosion behaviour of Fe-17Cr stainless steel in acid and alkaline solutions, *Tribology International*, vol. 32, n° 6, p. 295-303, 1999.
- [5] S. Mischler, Triboelectrochemical techniques and interpretation methods in tribocorrosion: A comparative evaluation, *Tribology International*, vol. 41, n° 7, p. 573-583, 2008.
- [6] S. W. Watson, F. J. Friedersdorf, B. W. Madsen, et S. D. Cramer, Methods of measuring wear-corrosion synergism, *Wear*, vol. 181-183, Part 2, n° 0, p. 476-484, 1995.
- [7] Y. Huang, X. Jiang, et S. Li, Pure mechanical wear loss measurement in corrosive wear, *Bulletin of Materials Science*, vol. 23, n° 6, p. 539-542, 2000.
- [8] D. Landolt, S. Mischler, et M. Stemp, Electrochemical methods in tribocorrosion: a critical appraisal, *Electrochimica Acta*, vol. 46, n° 24-25, p. 3913-3929, 2001.
- [9] S. Akonko, D. Y. Li, et M. Ziomek-Moroz, Effects of cathodic protection on corrosive wear of 304 stainless steel, *Tribology Letters*, vol. 18, n° 3, p. 405-410, 2005.
- [10] S. Tao et D. Y. Li, Investigation of corrosion-wear synergistic attack on nanocrystalline Cu deposits, *Wear*, vol. 263, n° 1-6, p. 363-370, 2007.
- [11] P. L. Wong, P. Huang, et Y. Meng, The Effect of the Electric Double Layer on a Very Thin Water Lubricating Film, *Tribology Letters*, vol. 14, n° 3, p. 197-203, 2003.
- [12] J. Geringer, B. Normand, C. Alemany-Dumont, et R. Diemiaszonek, Assessing the tribocorrosion behaviour of Cu and Al by electrochemical impedance spectroscopy, *Tribology International*, vol. 43, n° 11, p. 1991-1999, 2010.
- [13] I. Olefjord et L. Wegelius, Surface analysis of passive state, *Corrosion Science*, vol. 31, p. 89-98, 1990.
- [14] Techniques Giving Mechanistic Information, in *Techniques and Mechanisms in Electrochemistry*, Springer Netherlands, 1994, p. 36-227.
- [15] D. H. Buckley, *Surface Effects in Adhesion, Friction, Wear, and Lubrication*. Elsevier, 1981.
- [16] I. García, D. Drees, et J.P. Celis, Corrosion-wear of passivating materials in sliding contacts based on a concept of active wear track area, *Wear*, vol. 249, n° 5-6, p. 452-460, 2001.
- [17] X. Y. Wang et D. Y. Li, Application of an electrochemical scratch technique to evaluate contributions of mechanical and electrochemical attacks to corrosive wear of materials, *Wear*, vol. 259, n° 7-12, p. 1490-1496, 2005.